Research Square

Preprints are preliminary reports that have not undergone peer review.
They should not be considered conclusive, used to inform clinical practice,
or referenced by the media as validated information.

Resting-State EEG Theta-Band Functional Connectivity Characterizes Heterogeneity in Internet Gaming Disorder

Shichen Zhang
Central China Normal University
Yayun Meng
1242200479@qq.com

The Fifth People's Hospital of Nanning

Research Article

Keywords: Internet gaming disorder, theta oscillations, amplitude envelope correlation, representational similarity analysis, resting-state EEG

Posted Date: November 1st, 2026

DOI: https://doi.org/10.21203/rs.3.rs-11330610/v1

License: This work is licensed under a Creative Commons Attribution 4.0 International License.
Read Full License

Additional Declarations: No competing interests reported.

Abstract

Background.

Symptom-based assessments capture IGD severity but provide limited information about neurophysiological heterogeneity. We examined whether resting-state EEG amplitude envelope correlation (AEC) profiles relate to IGD symptoms and reveal connectivity-defined heterogeneity.

Methods.

Thirty participants with IGD and thirty healthy controls underwent five-minute eyes-closed resting-state EEG. Source-level AEC was estimated across theta, alpha, beta, and gamma bands. Exploratory representational similarity analysis tested associations between connectivity-profile dissimilarity and IGD-20 differences; theta-AEC profiles within IGD were further examined using principal component analysis and k-means clustering.

Results.

Within IGD, theta-AEC dissimilarity was associated with mood-modification differences (r = 0.277, p_{FDR} = 0.020), whereas the corresponding association in controls was not significant. Exploratory clustering indicated connectivity heterogeneity, with the largest difference involving Visual–Salience/Ventral Attention connectivity; clusters did not differ in IGD-20 scores or weekly gaming time.

Conclusions.

Theta-AEC may capture symptom-related neurophysiological variation within IGD.

1. Introduction

Internet gaming disorder (IGD) is an increasingly recognized mental health concern characterized by persistent and poorly controlled gaming behavior that results in clinically significant functional impairment (APA, 2013). Reflecting the growing recognition of disordered gaming, gaming disorder has been formally included as a disorder due to addictive behaviors in the eleventh revision of the International Classification of Diseases (ICD-11), whereas IGD remains listed in the DSM-5 as a condition warranting further research (APA, 2013; WHO, 2019). Epidemiological estimates vary considerably across populations, assessment instruments, and diagnostic thresholds, although problematic gaming and IGD appear to affect a non-negligible proportion of the population, particularly adolescents and young adults (Gopali et al., 2023; Limone et al., 2023; Long et al., 2018). Current diagnostic frameworks identify IGD primarily from behavioral symptoms and associated functional impairment, while empirical studies commonly quantify symptom severity using standardized self-report instruments such as the

IGD-20 Test (APA, 2013; Shu et al., 2019; WHO, 2019). Although these approaches are essential for clinical assessment, symptom-based classifications do not directly characterize the neural mechanisms underlying IGD and may provide limited resolution of its neurobiological heterogeneity (Insel et al., 2010; Yao et al., 2017; Zhang & Brand, 2018). Objective neurophysiological measures may therefore complement existing assessments by identifying neural features associated with individual symptom variation and supporting a more biologically informed characterization of IGD (Gil Ávila et al., 2023; Insel, 2014; Woo et al., 2017).

Resting-state EEG provides a means of examining intrinsic neural activity and functional connectivity across multiple frequency bands. Previous studies of IGD have reported connectivity differences spanning theta, alpha, beta, and gamma frequencies. Source-level analyses have identified increased theta, alpha, and beta connectivity within the default mode network and increased alpha and beta connectivity within a reward–salience network (Lee et al., 2022), whereas scalp EEG studies have reported increased beta and gamma coherence (Park et al., 2018). Together, these findings support examining resting-state connectivity across multiple frequency bands as a means of characterizing neural variation in IGD.

Within this multiband framework, theta oscillations (4–8 Hz) are of particular interest because of their involvement in cognitive control and coordination between prefrontal regions (Cavanagh et al., 2009). Evidence from IGD also supports their clinical relevance: a longitudinal study found that higher baseline resting-state theta power was associated with greater symptom improvement following treatment (Kim et al., 2017). Theta activity has additionally been implicated in affective regulation, with frontal theta power increasing during cognitive reappraisal of negative stimuli and correlating with reported regulation success (Ertl et al., 2013). This affective role provides a rationale for considering mood modification, an IGD-20 dimension concerning the use of gaming to alter affective states, among the symptom dimensions potentially related to theta activity (Pontes et al., 2014). Together, these findings provide a rationale for considering theta connectivity within a broader investigation of frequency-specific neural variation in IGD.

Amplitude envelope correlation (AEC) quantifies functional coupling by measuring the temporal covariation of band-limited signal envelopes between brain regions. Studies using source-reconstructed MEG have shown that amplitude-envelope-based connectivity can provide comparatively reproducible estimates of large-scale network organization, particularly when spatial leakage and shared zero-lag signals are appropriately controlled (Colclough et al., 2016; Hipp et al., 2012; Pourmotabbed et al., 2022). In IGD, resting-state functional connectivity studies have reported altered interactions within and between large-scale networks, including the default mode, salience, reward-related, and frontoparietal systems (Yan et al., 2021; Lee et al., 2022). Previous work has emphasized group-level connectivity differences and associations between selected connectivity measures and clinical severity. A complementary question is whether dissimilarity between individuals' whole-brain AEC profiles corresponds to differences in overall symptom severity and specific symptom dimensions across frequency bands.

In addition to examining how connectivity varies with symptoms, characterizing heterogeneity within IGD requires considering whether individuals exhibit distinct configurations of neural connectivity. Most neuroimaging studies of IGD have predominantly compared individuals with IGD against healthy controls, an approach that may obscure distinct patterns of neural organization within the IGD group (Yao et al., 2017; Zhang & Brand, 2018). Connectivity-based studies in other psychiatric conditions have identified candidate subgroups in depression, schizophrenia, post-traumatic stress disorder, and attention-deficit/hyperactivity disorder, raising the possibility that clinically defined diagnostic groups may contain multiple patterns of neural dysfunction (Bu et al., 2025; Drysdale et al., 2017; Li et al., 2022; Liu et al., 2021; Zhang et al., 2021). However, the stability and generalizability of such subgroup solutions remain active methodological concerns, as some influential connectivity-based biotypes have not been reproduced in independent samples (Dinga et al., 2019). This question is particularly relevant to IGD, given the variability in motivational, affective, and cognitive characteristics among individuals meeting diagnostic or screening criteria (Wang & Cheng, 2022; Zhao et al., 2026). It therefore remains unknown whether AEC profiles reveal connectivity-defined groupings within IGD and how such groupings relate to conventional clinical and behavioral characteristics.

The present study investigated resting-state functional connectivity heterogeneity within IGD through complementary dimensional and exploratory clustering analyses. Building on evidence of altered resting-state connectivity and its clinical associations in IGD, we evaluated the hypothesis that greater inter-individual dissimilarity in connectivity profiles would be associated with larger differences in IGD symptom scores. Representational similarity analysis (RSA) was used to examine this correspondence for IGD-20 total and subscale scores across theta, alpha, beta, and gamma bands, with parallel analyses in healthy controls providing a descriptive comparison. Theta connectivity was of particular interest given previous findings in IGD and the involvement of theta oscillations in cognitive-affective control. To further characterize neural variation within IGD, principal component analysis (PCA) and k-means clustering were applied to theta-AEC profiles to explore connectivity-defined groupings. These groupings were characterized using network-level connectivity summaries and clinical and behavioral measures. Figure 1 outlines the data analysis pipeline.

2. Methods

2.1 Participants and Procedures

Sixty adults were included in the study: 30 participants with internet gaming disorder (IGD) and 30 healthy controls (HCs). Participants were recruited through university notice boards and online advertisements. Eligibility for the IGD group required meeting at least five of the nine DSM-5 IGD criteria and reporting more than 30 hours of online gaming per week. IGD group assignment was based on the study screening criteria and was not confirmed by a clinician. Eligibility for the HC group required meeting none of the nine DSM-5 IGD criteria, reporting more than five hours of online gaming per week, and having no current or past psychiatric diagnosis (APA, 2013). Gaming-related symptom severity was assessed in both groups using the IGD-20 Test (Pontes et al., 2014). Exclusion criteria for both groups

included a history of neurological disorder, significant head injury, current psychotropic medication use, and uncorrected visual or auditory impairment. No a priori power analysis was conducted because the study was exploratory and the primary analyses relied on permutation-based representational similarity analysis and exploratory clustering. The target sample size was set at 30 participants per group before the present analyses, based on the available recruitment resources and eligibility criteria. Data collection ceased once 30 eligible participants had been enrolled in each group. To reduce reliance on parametric assumptions in the primary brain–behavior analysis, statistical significance was evaluated using 10,000 participant-label permutations, with false discovery rate correction applied across the prespecified tests. The study was approved by the institutional review board of the ethics committee of the first author's institution. The procedures were carried out according to the Declaration of Helsinki. All participants were informed about the study and provided informed consent. Participants completed the study questionnaires and an eyes-closed resting-state EEG recording.

Resting-state EEG was recorded during a five-minute eyes-closed condition. Participants were seated in a sound-attenuated, electrically shielded recording room and instructed to remain still, relax, and avoid deliberate mental activity. A brief practice period preceded the recording to ensure compliance with task instructions. EEG recordings were conducted between 09:00 and 17:00.

2.2 Measures

Internet Gaming Disorder Scale (IGD-20)

IGD-20. The IGD-20 Test is a 20-item self-report questionnaire assessing gaming-related symptom severity across six subscales (Pontes et al., 2014). Representative items include salience ("I usually think about my next gaming session when I am not playing"); mood modification ("I play games to help me cope with any bad feelings I might have"); tolerance ("I need to spend increasing amounts of time engaged in playing games"); withdrawal ("I feel sad if I am not able to play games"); conflict ("I believe my gaming is negatively impacting on important areas of my life"); and relapse ("I often try to play games less but find I cannot"). Each item is rated on a five-point Likert scale ranging from 1 (strongly disagree) to 5 (strongly agree), yielding a total score and six subscale scores. Previous studies have reported evidence supporting the reliability and validity of the IGD-20 Test (Pontes et al., 2014; Shu et al., 2019).

Depression Anxiety Stress Scale (DASS-21)

DASS-21. The Depression Anxiety Stress Scales–21 (DASS-21) is a widely used 21-item measure assessing the severity of depression, anxiety, and stress symptoms over the preceding week. DASS-21 total scores were used to characterize overall psychological distress and were compared between the IGD and HC groups (Lu et al., 2018; Zhang et al., 2024).

2.3 EEG Recording

EEG was recorded using a 64-channel BrainProducts actiCHamp system with active Ag/AgCl electrodes arranged according to the extended 10–20 international system. The reference electrode was placed at FCz and re-referenced offline. Electrode impedances were maintained below 10 kΩ for all channels throughout the recording. EEG was amplified and digitized at a sampling rate of 1,000 Hz, and a hardware bandpass filter of 0.1–250 Hz was applied during acquisition. Electrode positions were digitized during acquisition; however, source reconstruction in the present analysis used standard electrode coordinates.

2.4 EEG Preprocessing and Feature Extraction

Raw EEG data were preprocessed using the DISCOVER-EEG pipeline (v1.1.0), an open-source, fully automated pipeline designed for biomarker discovery in resting-state EEG data (Gil Ávila et al., 2023). Raw data were converted to Brain Imaging Data Structure (BIDS) format before processing and were downsampled to 250 Hz within the pipeline. Line noise was removed with the CleanLine plugin (Mullen, 2012) at the frequency specified in the recording metadata. Bad channels were identified and rejected using pop_clean_rawdata. The data were high-pass filtered with a transition band of 0.25–0.75 Hz and re-referenced to the common average. Independent component analysis was performed with runica and repeated ten times per recording to reduce ICA non-determinism. Components classified by ICLabel (Pion-Tonachini et al., 2019) with a probability greater than 80% of representing eye or muscle artefacts were removed. Rejected channels were interpolated using spherical splines. Bad time segments were removed using pop_clean_rawdata and BurstRejection enabled. The run whose clean-sample mask was closest to the average mask across the ten repetitions was selected for subsequent analysis. Finally, cleaned continuous data were segmented into artefact-free 2-s epochs with 50% overlap, and epochs containing ASR-induced discontinuities were rejected.

Spectral and connectivity features were extracted using the DISCOVER-EEG pipeline (Gil Ávila et al., 2023). For each epoch, power spectral density was computed with Slepian multitaper spectral estimation, then averaged across epochs and channels to obtain a grand average spectrum for each participant. Band-specific power was computed for theta (4–8 Hz), alpha (8–13 Hz), beta (13–30 Hz), and gamma (30–45 Hz). Band-specific source reconstruction used linearly constrained minimum variance beamforming with a standard boundary-element head model and standard electrode coordinates. Sources were positioned at the centroids of the 100 Schaefer cortical parcels with seven-network assignments (Schaefer et al., 2018). Beamformer settings included 5% regularization, fixed source orientation, and array-gain weight normalization. AEC was computed from Hilbert-transformed source signals after pairwise orthogonalization to reduce zero-lag signal leakage. Pearson correlations between log-transformed power envelopes were averaged across both orthogonalization directions, normalized by 0.577, and averaged across epochs. The 4950 unique off-diagonal connections were vectorized for subsequent analyses.

2.5 Statistical Analysis

Demographic and clinical comparisons. Demographic and clinical characteristics were compared between the IGD and HC groups using two-sided independent-samples t tests for continuous variables and a chi-square test for sex distribution. All tests were two-tailed, with an alpha level of 0.05. Continuous variables are reported as mean ± standard deviation. Cohen's d was calculated using the pooled sample standard deviation, and 95% confidence intervals were reported for mean differences calculated as IGD minus HC. The Benjamini–Hochberg procedure was applied across eight scale comparisons: IGD-20 total score, its six subscale scores, and DASS-21 total score. Demographic comparisons and weekly gaming time were reported with unadjusted p values.

Representational similarity analysis.

RSA was used to examine whether inter-individual differences in whole-brain AEC connectivity were associated with differences in IGD-20 scores. Analyses were conducted separately within the IGD and HC groups. For each frequency band, each of the 4950 AEC features was z-standardized across participants within each group. A neural representational dissimilarity matrix was then constructed by calculating the Euclidean distance between every pair of participants' standardized AEC profiles.

Behavioral dissimilarity matrices were constructed from the absolute pairwise differences in the IGD-20 total score and its six subscale scores: salience, mood modification, tolerance, withdrawal symptoms, conflict, and relapse. The association between each neural and behavioral dissimilarity matrix was quantified using Spearman rank correlation between their upper-triangular elements.

Statistical significance was evaluated using 10000 participant-label permutations. In each permutation, the rows and corresponding columns of the behavioral dissimilarity matrix were permuted jointly, preserving its internal dependency structure. Two-sided empirical p values were calculated as the proportion of permuted correlation coefficients whose absolute values were at least as large as the absolute observed coefficient. The Benjamini–Hochberg procedure was applied separately within each group across the 28 AEC tests formed by four frequency bands and seven IGD-20 variables (Benjamini & Hochberg, 1995).

These focused AEC analyses followed a broader exploratory screen involving multiple neural feature classes in the same sample. Accordingly, the AEC analyses were treated as exploratory follow-up analyses rather than independent confirmatory tests. Analyses in the HC group provided a descriptive comparison of the pattern of associations; because the present analysis did not directly test the difference between group-specific RSA coefficients, significance in one group and non-significance in the other was not interpreted as evidence of a statistically significant group interaction.

Exploratory edgewise follow-up analysis

To explore the anatomical distribution of the theta-AEC association with mood modification, a separate edgewise analysis was conducted within the IGD group. For each of the 4950 connections, the AEC value was correlated with the IGD-20 mood-modification score across participants using Spearman rank

correlation. The resulting p values were corrected across all connections using the Benjamini–Hochberg procedure. The nominal p value for each connection was obtained from the conventional Spearman correlation test; no edgewise permutation test was performed. Network affiliations were assigned according to the seven-network Schaefer atlas, and mean signed and absolute correlation coefficients were calculated within and between networks for descriptive visualization. This analysis was distinct from the whole-brain RSA and was considered exploratory; it did not constitute a decomposition of the RSA coefficient.

Exploratory cluster identification

Exploratory clustering was performed on the theta-band AEC profiles of participants with IGD. The 4,950 connectivity features were standardized across participants and subjected to principal component analysis, with sufficient components retained to explain at least 95% of the total variance. Candidate cluster numbers were evaluated using the gap statistic for k = 1–8, based on 50 uniformly distributed reference datasets, and the mean Silhouette coefficient for k = 2–6. Because the two criteria yielded different solutions, with the gap statistic favoring k = 4 and the Silhouette coefficient favoring k = 2, the two-cluster solution was retained as a parsimonious exploratory representation rather than regarded as a uniquely optimal solution. K-means clustering was performed in the PCA-reduced space using 200 initializations and a fixed random seed.

After clustering, mean connectivity was calculated for each pair of the seven large-scale networks. The cluster with lower mean Visual–Salience/Ventral Attention connectivity was labelled Cluster 1, and the cluster with higher connectivity was labelled Cluster 2. This labelling was performed post hoc for descriptive interpretation and was not used to determine the cluster assignments. Differences between the two clusters in weekly gaming time, IGD-20 total score, and the six IGD-20 subscale scores were evaluated using two-sided Mann–Whitney U tests. Cohen's d was additionally reported as a descriptive standardized effect-size measure. Given the exploratory nature of these comparisons and the small sample size, non-significant results were not interpreted as evidence that the clusters were equivalent or behaviorally indistinguishable.

3. Results

3.1 Demographic and Clinical Characteristics

Table 1
Demographic and clinical characteristics of the participants.

Variables	IGD (M ± SD)	HCs (M ± SD)	*t/χ2*	*p*
Age(years)	20.40 ± 1.99	19.80 ± 1.83	1.215	0.229
Male/Female	14/16	15/15	0.067	0.796
Education(years)	14.77 ± 2.64	14.47 ± 1.36	0.554	0.581
Game Duration (Hours/Week)	37.07 ± 3.42	18.00 ± 4.06	19.665	< 0.001
IGD total score	73.40 ± 2.67	35.80 ± 3.03	50.940	< 0.001
salience	11.30 ± 1.26	5.47 ± 1.04	19.511	< 0.001
mood modification	12.90 ± 1.32	6.80 ± 1.19	18.810	< 0.001
tolerance	11.10 ± 1.30	5.03 ± 0.85	21.439	< 0.001
withdrawal	10.43 ± 1.19	5.13 ± 0.94	19.122	< 0.001
conflict	16.80 ± 1.83	8.20 ± 1.42	20.335	< 0.001
relapse	10.87 ± 0.82	5.17 ± 1.02	23.864	< 0.001
DASS total score	21.90 ± 5.89	12.80 ± 4.63	6.649	< 0.001

Data are presented as mean ± standard deviation unless otherwise indicated. Sex distribution is presented as the number of male/female participants. Group differences were assessed using independent-samples t-tests for continuous variables and a chi-square test for sex. IGD-20, 20-item Internet Gaming Disorder Test; DASS, Depression Anxiety Stress Scales.

Demographic characteristics were first compared between the IGD and HC groups. The chi-square test showed no significant difference in sex distribution between the groups ($\chi^2 = 0.067$, $p = 0.796$). Independent-samples t-tests also showed no significant group differences in age (IGD: 20.40 ± 1.99 years; HC: 19.80 ± 1.83 years; $t = 1.215$, $p = 0.229$) or years of education (IGD: 14.77 ± 2.64 years; HC: 14.47 ± 1.36 years; $t = 0.554$, $p = 0.581$). Participants with IGD reported substantially more weekly gaming time than HCs (37.07 ± 3.42 vs. 18.00 ± 4.06 hours/week; $t = 19.665$, $p < 0.001$, Cohen's $d = 5.08$, 95% CI [17.13, 21.01]). They also had higher IGD-20 total scores (73.40 ± 2.67 vs. 35.80 ± 3.03; $t = 50.940$, $p < 0.001$, Cohen's $d = 13.15$, 95% CI [36.12, 39.08]). Independent-samples t-tests were subsequently used to compare the six IGD-20 dimensions and DASS total scores between the groups. Figure 2 illustrates the observed differences across these measures. After false discovery rate correction, participants with IGD showed significantly higher scores for salience ($t = 19.511$, $p_{FDR} = 6.43 \times 10^{-27}$, Cohen's $d = 5.04$, 95% CI [5.23, 6.43]), mood modification ($t = 18.810$, $p_{FDR} = 2.70 \times 10^{-26}$, Cohen's $d = 4.86$, 95% CI [5.45, 6.75]), tolerance ($t = 21.439$, $p_{FDR} = 1.05 \times 10^{-28}$, Cohen's $d = 5.54$, 95% CI [5.50, 6.63]), withdrawal symptoms ($t = 19.122$, $p_{FDR} = 1.42 \times 10^{-26}$, Cohen's $d = 4.94$, 95% CI [4.75, 5.85]), conflict ($t = 20.335$, $p_{FDR} = 1.05 \times 10^{-27}$, Cohen's $d = 5.25$, 95% CI [7.75, 9.45]), relapse ($t = 23.864$, $p_{FDR} = 7.80 \times 10^{-31}$, Cohen's $d = 6.16$, 95% CI

[5.22, 6.18]), and DASS total score (t = 6.649, p_{FDR} = 1.14 × 10^{-8}, Cohen's d = 1.72, 95% CI [6.36, 11.84]) than HCs. Descriptive statistics for all measures are summarized in Table 1.

3.2 RSA of theta-AEC and IGD-20 mood-modification scores

Exploratory RSA examined associations between AEC connectivity dissimilarity and IGD-20 score dissimilarity across four frequency bands within each group. The IGD-20 total score and six subscale scores yielded 28 tests per group. These analyses followed a broader exploratory screen of neural feature classes in the same sample.

Within the IGD group, theta-AEC connectivity patterns covaried significantly with the IGD-20 mood modification subscale (r_s = 0.277, p_{FDR} = 0.020; Fig. 3a). No other frequency band–behavioral variable combination survived FDR correction within the IGD group (Fig. 3b). Theta-AEC dissimilarity was not significantly associated with dissimilarity in IGD-20 total scores (r_s = − 0.048, p_{perm} = 0.559). Participants with more similar theta-AEC profiles therefore tended to have more similar mood-modification scores.

Within the HC group, the corresponding theta-AEC association with mood-modification scores was not significant (r = −0.081, p_{perm} = 0.287). Gamma-AEC dissimilarity was associated with dissimilarity in IGD-20 total scores (r = 0.342, p_{FDR} = 0.042) and relapse scores (r = 0.291, p_{FDR} = 0.042; Fig. 3b). Differences between group-specific RSA coefficients were not directly tested.

An exploratory edgewise analysis examined associations between theta-AEC values and IGD-20 mood-modification scores within the IGD group. Of the 4950 connections tested, 42 met the uncorrected threshold of p < 0.05, but none survived FDR correction. Network summaries of mean signed and mean absolute edgewise correlations are shown in Fig. 4a and Fig. 4b, respectively. The largest positive edgewise correlations involved individual Salience/Ventral Attention–Default Mode and Frontoparietal–Default Mode connections (r = 0.360, unadjusted p = 0.051; r = 0.343, unadjusted p = 0.064, respectively). Neither association reached nominal statistical significance. Mean signed correlations were negative across all within- and between-network categories. These summaries were descriptive and did not identify statistically significant network-specific associations or constitute a decomposition of the whole-brain RSA result.

3.3 Exploratory Theta-AEC Clustering

3.3.1 Cluster Identification and Connectivity Profiles

Exploratory clustering was performed to examine whether theta-AEC profiles supported a parsimonious grouping within the IGD sample. PCA retained 23 components that collectively explained 95.2% of the variance. The gap statistic selected k = 4, whereas the mean Silhouette coefficient was highest at k = 2 (Silhouette = 0.313; Fig. 5a). Given the disagreement between the two criteria and the small sample size, the two-cluster solution was retained as an exploratory, parsimonious representation rather than a

uniquely optimal solution. Cluster 1 comprised 16 participants and Cluster 2 comprised 14 participants. For visualization, the first two principal components explained 58.9% and 5.2% of the variance, respectively (Fig. 5b). Post hoc network-level summaries showed consistently lower mean AEC values in Cluster 1 than in Cluster 2, with the largest difference observed for Visual–Salience/Ventral Attention connectivity (Cluster 1 minus Cluster 2 = − 0.062; Fig. 5c). The clusters were therefore labelled as the lower and higher Visual–Salience/Ventral Attention connectivity groups for descriptive purposes.

3.3.2 No Significant Behavioral Differences Between Theta-AEC Clusters

Table 2
Clinical and behavioral comparisons between theta-AEC clusters

Behavioral Variable	**Cluster 1 (Mean ± SD)**	**Cluster 2 (Mean ± SD)**	**Mann-Whitney U**	***p***
Weekly Game Time	37.12 ± 3.44	37.00 ± 3.53	115.5	0.898
IGD Score	73.12 ± 2.25	73.71 ± 3.15	106.5	0.833
Salience	11.44 ± 1.03	11.14 ± 1.51	129	0.470
Mood modification	13.12 ± 1.15	12.64 ± 1.50	137	0.286
Tolerance	10.75 ± 1.13	11.50 ± 1.40	80	0.176
Withdrawal	10.31 ± 1.30	10.57 ± 1.09	100.5	0.638
Conflict	16.69 ± 1.35	16.93 ± 2.30	97.5	0.552
Relapse	10.81 ± 0.98	10.93 ± 0.62	104	0.740

Exploratory Mann–Whitney U tests found no statistically significant differences between the two clusters in weekly gaming time, IGD-20 total score, or any of the six IGD-20 subscale scores (all $p \geq 0.05$; Table 2). Absolute Cohen's *d* values ranged from 0.036 to 0.590. Weekly gaming time was similar between Cluster 1 (37.12 ± 3.44 hours/week) and Cluster 2 (37.00 ± 3.53 hours/week; $U = 115.5$, $p = 0.898$). IGD-20 total scores also did not differ significantly (73.12 ± 2.25 vs. 73.71 ± 3.15; $U = 106.5$, $p = 0.833$). The difference in mood-modification scores was likewise not significant ($U = 137.0$, $p = 0.286$). These analyses did not provide evidence of behavioral differences between the clusters; however, non-significant tests were not interpreted as evidence of equivalence.

4. Discussion

The present study identifies resting-state theta-AEC as a multivariate correlate of heterogeneity within IGD at both continuous and subgroup levels. At the continuous level, inter-individual differences in whole-brain theta-AEC profiles were aligned with variation in IGD-20 mood-modification scores after correction

across the 28 AEC analyses. At the subgroup level, theta-AEC profiles supported a parsimonious two-cluster representation characterized by broadly lower and higher connectivity patterns, while the measured gaming and IGD-20 variables did not differ significantly between the clusters. Together, these analyses describe mood-modification-related variation and exploratory connectivity groupings within the IGD sample. By combining RSA with exploratory clustering, the study provides a network-level framework for characterizing both continuous mood-modification-related variation and connectivity heterogeneity within IGD.

The correspondence between theta-AEC dissimilarity and IGD-20 mood-modification scores links distributed resting-state theta connectivity to an affect-related dimension of IGD. Mood modification describes the use of gaming to alter subjective mood and is one of the six components assessed by the IGD-20 Test (Pontes et al., 2014). Although it was not designed as a general measure of emotion regulation, this construct is relevant to affective processes implicated in problematic gaming. Studies using dedicated emotion-regulation measures have similarly reported poorer emotional adjustment among individuals with IGD (Lin et al., 2020). The association observed in the theta band is consistent with evidence linking frontal theta activity to cognitive control and emotion regulation (Cavanagh & Frank, 2014). Frontal theta increases during cognitive reappraisal, and task-related theta power has been associated with reported regulation success (Ertl et al., 2013). Cross-species evidence further shows that low-frequency prefrontal activity can coordinate distributed circuits involved in affective behavior, including prefrontal–amygdala coupling during fear-related states (Karalis et al., 2016). Together, these findings position theta-AEC as a candidate network-level signature of mood-modification-related variation in IGD and provide a resting-state complement to previous task-based observations.

The broader pattern of RSA associations provides additional context for the theta–mood-modification finding. Theta-AEC dissimilarity was associated with mood-modification score differences within the IGD group but not within HCs, whereas gamma-AEC dissimilarity in HCs was associated with variation in IGD-20 total and relapse scores. These results indicate that the behavioral dimensions tracked by resting-state AEC may vary across frequency bands and participant groups. In particular, theta connectivity may be relevant to mood-related gaming tendencies among individuals meeting IGD criteria, whereas gamma connectivity may track other forms of gaming-related variation among HCs. This interpretation is compatible with models in which affective responses, coping expectancies, and reinforcement processes interact in the maintenance of problematic gaming (Brand et al., 2016; Melodia et al., 2022). Because the group-specific RSA coefficients were not directly compared, however, the observed pattern should be understood as a descriptive frequency- and group-dependent configuration rather than a statistically established group interaction or disorder-transition mechanism.

The edgewise analysis further clarifies the level at which the theta-AEC association was expressed. Although the whole-connectivity-profile RSA survived correction, none of the 4950 individual edgewise associations survived FDR correction. Two of the largest positive correlations involved individual Salience/Ventral Attention–Default Mode and Frontoparietal–Default Mode connections, but neither reached nominal significance. Moreover, descriptive network aggregation showed negative mean signed

correlations across all within- and between-network categories, with absolute correlations distributed broadly across the seven-network architecture. The findings therefore do not support localization of the RSA association to a specific connection or network pair. Instead, the contrast between the whole-profile RSA and the edgewise results highlights the potential value of multivariate representational geometry for detecting coordinated inter-individual variation that may not be recoverable from mass-univariate connection tests (Kriegeskorte et al., 2008; Kriegeskorte & Kievit, 2013). This network-wide sensitivity may be useful when developing candidate connectivity measures of heterogeneous clinical features, although its reproducibility must be established in independent samples.

The exploratory clustering analysis complements the dimensional RSA result by examining whether theta-AEC heterogeneity also supports a parsimonious grouping within IGD. The retained two-cluster representation was characterized by broadly lower theta-AEC connectivity in Cluster 1 than in Cluster 2, with the largest network-level difference involving Visual–Salience/Ventral Attention connectivity. This pattern may be relevant to individual variation in the integration of visual processing and salience allocation. Previous behavioral, electrophysiological, and neuroimaging studies have shown that individuals with IGD can exhibit altered attentional processing of gaming-related visual cues and increased responses within visual and attentional-control regions (Zhang et al., 2016; Kim et al., 2018). The present resting-state result cannot establish cue reactivity directly, but it identifies Visual–Salience/Ventral Attention coupling as a focused hypothesis for subsequent task-based investigation. None of the measured gaming variables differed significantly between the two clusters, indicating that the observed connectivity separation was not accompanied by detectable differences in IGD-20 scores or weekly gaming time in this sample. More broadly, this dimensional-plus-clustering approach is consistent with efforts to characterize psychiatric heterogeneity using resting-state connectivity, while positioning the present clusters as candidate neural phenotypes rather than validated clinical subtypes (Zhang et al., 2021).

Several limitations define the scope of the present findings. First, the relatively small IGD sample (n = 30) limits the stability and generalizability of the clustering solution. This is particularly relevant because the Silhouette coefficient favored two clusters, whereas the gap statistic favored four. The two-cluster representation should therefore be regarded as an exploratory description of theta-AEC heterogeneity until it is reproduced using resampling-based stability analyses and an independent cohort. Second, the focused AEC analyses followed a broader exploratory screen, and the RSA coefficients obtained in the IGD and HC groups were not compared directly. Preregistered replication and formal between-group tests will be needed to determine whether the theta–mood-modification association differs reliably between groups. Third, mood modification reflects the use of gaming to alter subjective mood and is not a general measure of emotion-regulation ability. Future studies should therefore combine the IGD-20 with dedicated emotion-regulation measures and ecological assessments of affect-related gaming. Finally, the cross-sectional resting-state design cannot establish whether theta-AEC differences contribute to, result from, or change with the progression of IGD. Longitudinal studies incorporating gaming-cue tasks and intervention outcomes could clarify the functional and potential clinical relevance of the continuous and cluster-level connectivity patterns identified here.

5. Conclusion

This study identifies resting-state theta-band AEC as a candidate neural signature of heterogeneity within IGD. At the continuous level, inter-individual differences in whole-brain theta-AEC profiles were associated with variation in IGD-20 mood-modification scores. At the cluster level, theta-AEC profiles supported an exploratory two-cluster representation characterized most clearly by differences in Visual–Salience/Ventral Attention connectivity, while no significant differences were detected in the measured gaming-related variables. Together, these findings relate theta-AEC variation to mood modification and provide an exploratory description of connectivity heterogeneity within IGD. Resting-state theta-AEC therefore provides a focused neurophysiological framework for characterizing IGD heterogeneity and a promising candidate feature for future biologically informed stratification studies.

Declarations

Ethics approval

This study was approved by the Ethics Committee of the School of Psychology of Central China Normal University [Approval No. CCNU-IRB-202311009b; Approval date: November 8, 2023]. All procedures involving human participants were conducted in accordance with the ethical standards of the institutional research committee. Written informed consent was obtained from all participants prior to participation.

Consent to participate

Informed consent was obtained from all individual participants included in the study.

Conflict of interest

On behalf of all the authors, the corresponding author states that there are no conflicts of interest.

Funding Statement

This research did not receive any specific grant from funding agencies in the public, commercial, or not-for-profit sectors.

Author Contribution

Shichen Zhang contributed to the study design, investigation, data curation, formal analysis, and writing of the original draft. Yayun Meng contributed to the conceptualization, study design, supervision, and review and editing of the manuscript. All authors read and approved the final manuscript.

Data Availability

The data that support the findings of this study are available from the corresponding author upon reasonable request.

References

1. APA. Diagnostic and statistical manual of mental disorders (DSM-5®). Arlington, VA: American Psychiatric Pub; 2013.
2. Benjamini Y, Hochberg Y. Controlling the false discovery rate: a practical and powerful approach to multiple testing. J Roy Stat Soc: Ser B (Methodol). 1995;57(1):289–300.
3. Brand M, Young KS, Laier C, Wölfling K, Potenza MN. Integrating psychological and neurobiological considerations regarding the development and maintenance of specific Internet-use disorders: An Interaction of Person-Affect-Cognition-Execution (I-PACE) model. Neurosci Biobehavioral Reviews. 2016;71:252–66.
4. Bu X, Xia M, Cui Z, He Y. Toward individual heterogeneity and neurobiological subtypes in attention-deficit/hyperactivity disorder. J Pac Rim Psychol. 2025;19:18344909241308101.
5. Cavanagh JF, Cohen MX, Allen JJ. Prelude to and resolution of an error: EEG phase synchrony reveals cognitive control dynamics during action monitoring. J Neurosci. 2009;29(1):98–105.
6. Cavanagh JF, Frank MJ. Frontal theta as a mechanism for cognitive control. Trends Cogn Sci. 2014;18(8):414–21.
7. Colclough GL, Woolrich MW, Tewarie PK, Brookes MJ, Quinn AJ, Smith SM. How reliable are MEG resting-state connectivity metrics? NeuroImage. 2016;138:284–93.
8. Dinga R, Schmaal L, Penninx BW, van Tol MJ, Veltman DJ, van Velzen L, Marquand AF. Evaluating the evidence for biotypes of depression: Methodological replication and extension of. NeuroImage: Clin. 2019;22:101796.
9. Drysdale AT, Grosenick L, Downar J, Dunlop K, Mansouri F, Meng Y, Liston C. Resting-state connectivity biomarkers define neurophysiological subtypes of depression. Nat Med. 2017;23(1):28–38.
10. Ertl M, Hildebrandt M, Ourina K, Leicht G, Mulert C. Emotion regulation by cognitive reappraisal—the role of frontal theta oscillations. NeuroImage. 2013;81:412–21.
11. Gil Ávila C, Bott FS, Tiemann L, Hohn VD, May ES, Nickel MM, Ploner M. DISCOVER-EEG: an open, fully automated EEG pipeline for biomarker discovery in clinical neuroscience. Sci data. 2023;10(1):613.
12. Gopali L, Dhital R, Koirala R, Shrestha T, Bhusal S, Rimal R, Shah R. (2023). Effect of COVID-19 pandemic on internet gaming disorder among general population: A systematic review and meta-analysis. PLOS global public health, 3(4), e0001783.

13. Hipp JF, Hawellek DJ, Corbetta M, Siegel M, Engel AK. Large-scale cortical correlation structure of spontaneous oscillatory activity. Nat Neurosci. 2012;15(6):884–90.
14. Insel T, Cuthbert B, Garvey M, Heinssen R, Pine DS, Quinn K, Wang P. Research domain criteria (RDoC): toward a new classification framework for research on mental disorders. Am J Psychiatry. 2010;167(7):748–51.
15. Insel TR. The NIMH research domain criteria (RDoC) project: precision medicine for psychiatry. Am J Psychiatry. 2014;171(4):395–7.
16. Karalis N, Dejean C, Chaudun F, Khoder S, Rozeske RR, Wurtz H, Herry C. 4-Hz oscillations synchronize prefrontal–amygdala circuits during fear behavior. Nat Neurosci. 2016;19(4):605–12.
17. Kim SN, Kim M, Lee TH, Lee JY, Park S, Park M, Choi JS. Increased attentional bias toward visual cues in internet gaming disorder and obsessive-compulsive disorder: An event-related potential study. Front Psychiatry. 2018;9:315.
18. Kim YJ, Lee JY, Oh S, Park M, Jung HY, Sohn BK, Choi JS. Associations between prospective symptom changes and slow-wave activity in patients with Internet gaming disorder: a resting-state EEG study. Medicine. 2017;96(8):e6178.
19. Kriegeskorte N, Kievit RA. Representational geometry: integrating cognition, computation, and the brain. Trends Cogn Sci. 2013;17(8):401–12.
20. Kriegeskorte N, Mur M, Bandettini PA. Representational similarity analysis-connecting the branches of systems neuroscience. Front Syst Neurosci. 2008;2:249.
21. Lee JY, Choi CH, Park M, Park S, Choi JS. Enhanced resting-state EEG source functional connectivity within the default mode and reward-salience networks in internet gaming disorder. Psychol Med. 2022;52(11):2189–97.
22. Li Q, Coulson Theodorsen M, Konvalinka I, Eskelund K, Karstoft KI, Andersen B, S., Andersen TS. Resting-state EEG functional connectivity predicts post-traumatic stress disorder subtypes in veterans. J Neural Eng. 2022;19(6):066005.
23. Limone P, Ragni B, Toto GA. The epidemiology and effects of video game addiction: A systematic review and meta-analysis. Acta Psychol. 2023;241:104047.
24. Lin P-Y, Lin H-C, Lin P-C, Yen J-Y, Ko C-H. The association between emotional regulation and internet gaming disorder. Psychiatry Res. 2020;289:113060.
25. Liu Z, Palaniyappan L, Wu X, Zhang K, Du J, Zhao Q, Feng J. Resolving heterogeneity in schizophrenia through a novel systems approach to brain structure: individualized structural covariance network analysis. Mol Psychiatry. 2021;26(12):7719–31.
26. Long J, Liu T, Liu Y, Hao W, Maurage P, Billieux J. Prevalence and correlates of problematic online gaming: A systematic review of the evidence published in Chinese. Curr Addict Rep. 2018;5(3):359–71.
27. Lu S, Hu S, Guan Y, Xiao J, Cai D, Gao Z, Margraf J. (2018). Measurement invariance of the Depression Anxiety Stress Scales-21 across gender in a sample of Chinese university students. *Frontiers in psychology*, *9*, 2064.

28. Melodia F, Canale N, Griffiths MD. The role of avoidance coping and escape motives in problematic online gaming: A systematic literature review. Int J Mental Health Addict. 2022;20(2):996–1022.
29. Mullen T. (2012). CleanLine EEGLAB plugin. *San Diego, CA: Neuroimaging Informatics Toolsand Resources Clearinghouse (NITRC)*.
30. Park S, Ryu H, Lee JY, Choi A, Kim DJ, Kim SN, Choi JS. Longitudinal changes in neural connectivity in patients with internet gaming disorder: A resting-state EEG coherence study. Front Psychiatry. 2018;9:252.
31. Pion-Tonachini L, Kreutz-Delgado K, Makeig S. ICLabel: An automated electroencephalographic independent component classifier, dataset, and website. NeuroImage. 2019;198:181–97.
32. Pontes HM, Király O, Demetrovics Z, Griffiths MD. (2014). The conceptualisation and measurement of DSM-5 Internet Gaming Disorder: The development of the IGD-20 Test. PLoS ONE, 9(10), e110137.
33. Pourmotabbed H, de Jongh Curry AL, Clarke DF, Tyler-Kabara EC, Babajani-Feremi A. Reproducibility of graph measures derived from resting-state MEG functional connectivity metrics in sensor and source spaces. Hum Brain Mapp. 2022;43(4):1342–57.
34. Schaefer A, Kong R, Gordon EM, Laumann TO, Zuo XN, Holmes AJ, Yeo BT. Local-global parcellation of the human cerebral cortex from intrinsic functional connectivity MRI. Cereb Cortex. 2018;28(9):3095–114.
35. Shu M, Jacob YI, Xuan APM, Z., Anise MS, W. Psychometric validation of the Internet Gaming Disorder-20 Test among Chinese middle school and university students. J Behav addictions. 2019;8(2):295–305.
36. Wang HY, Cheng C. (2022). The associations between gaming motivation and internet gaming disorder: Systematic review and meta-analysis. JMIR mental health, 9(2), e23700.
37. WHO. (2019). International classification of diseases for mortality and morbidity statistics (11th revision). Retrieved from https://icd.who.int/browse/2024-01/mms/en#1448597234
38. Woo CW, Chang LJ, Lindquist MA, Wager TD. Building better biomarkers: brain models in translational neuroimaging. Nat Neurosci. 2017;20(3):365–77.
39. Yan H, Li Q, Yu K, Zhao G. Large-scale network dysfunction in youths with Internet gaming disorder: a meta-analysis of resting-state functional connectivity studies. Prog Neuropsychopharmacol Biol Psychiatry. 2021;109:110242.
40. Yao YW, Liu L, Ma SS, Shi XH, Zhou N, Zhang JT, Potenza MN. Functional and structural neural alterations in Internet gaming disorder: A systematic review and meta-analysis. Neurosci Biobehavioral Reviews. 2017;83:313–24.
41. Zhang JT, Brand M. Neural mechanisms underlying internet gaming disorder. Front Psychiatry. 2018;9:404.
42. Zhang Y, Lin X, Zhou H, Xu J, Du X, Dong G. Brain activity toward gaming-related cues in internet gaming disorder during an addiction Stroop task. Front Psychol. 2016;7:714.

43. Zhang Y, Wu W, Toll RT, Naparstek S, Maron-Katz A, Watts M, Etkin A. Identification of psychiatric disorder subtypes from functional connectivity patterns in resting-state electroencephalography. Nat biomedical Eng. 2021;5(4):309–23.
44. Zhang Z, Lin R, Qiu A, Wu H, Wu S, Zhang L, Zhou J. Application of DASS-21 in Chinese students: invariance testing and network analysis. BMC Public Health. 2024;24(1):2934.
45. Zhao H, Xiao Z, Li S, Liu J, He Q. (2026). Neural representations of dynamical state and trait impulsivity in individuals at risk for internet gaming disorder. Mol Psychiatry, 1–10.

Figures

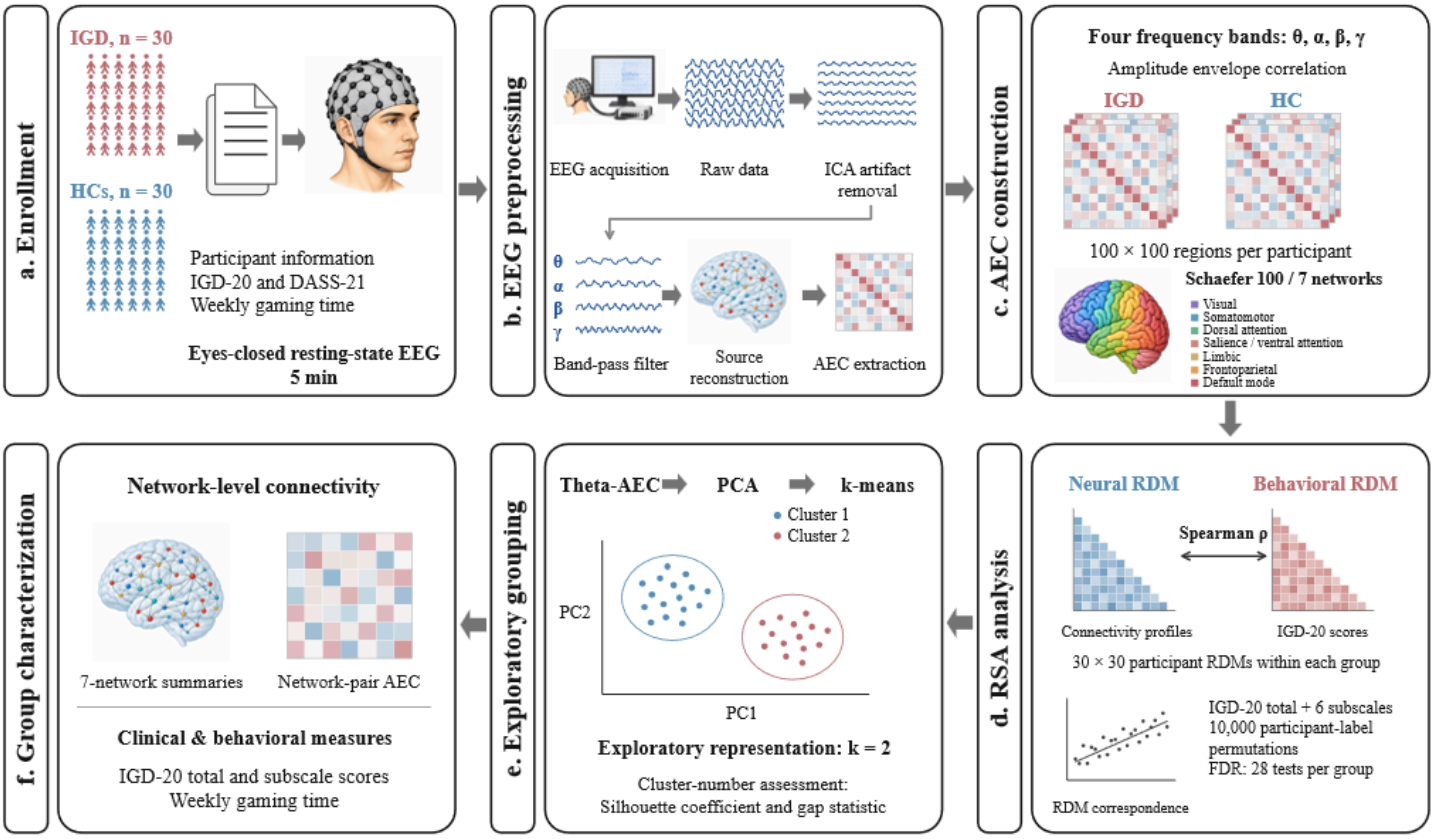


Figure 1

Schematic overview of the data analysis pipeline. The procedure consisted of six parts: (a) participant enrollment; (b) EEG preprocessing; (c) AEC connectivity construction; (d) RSA of connectivity profiles and IGD-20 scores; (e) exploratory clustering of theta-AEC profiles within IGD; and (f) network-level, clinical, and behavioral characterization of the resulting groups. Connectivity was computed using the 100-region Schaefer parcellation across theta, alpha, beta, and gamma bands. RSA was performed separately in IGD and HCs, whereas clustering used PCA and k-means. IGD, internet gaming disorder; HCs, healthy controls; EEG, electroencephalography; AEC, amplitude envelope correlation; RSA, representational similarity analysis; PCA, principal component analysis; ICA, independent component

analysis; RDM, representational dissimilarity matrix; FDR, false discovery rate; DASS-21, 21-item Depression Anxiety Stress Scales.

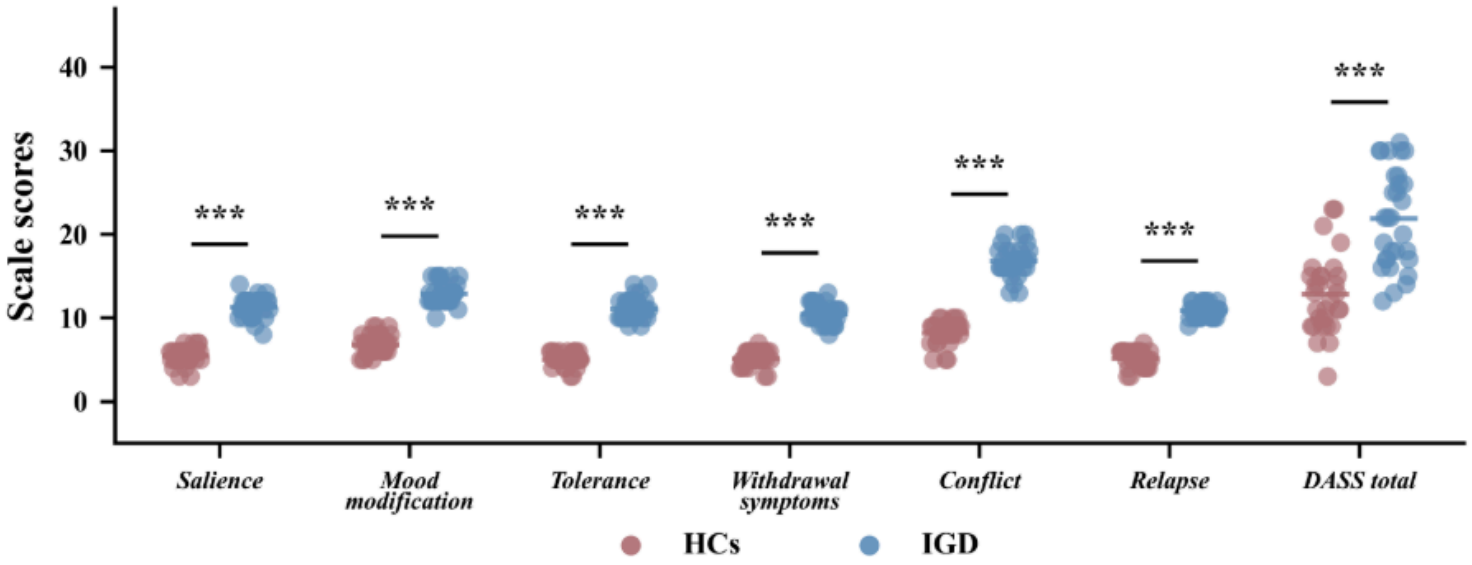


Figure 2

Group differences in IGD-20 subscale scores and DASS-21 total scores. Each dot represents one participant, and horizontal lines indicate group means. Red denotes healthy controls (HCs), and blue denotes participants with internet gaming disorder (IGD). *** denotes $p_{FDR} < 0.001$. DASS, Depression Anxiety Stress Scales.

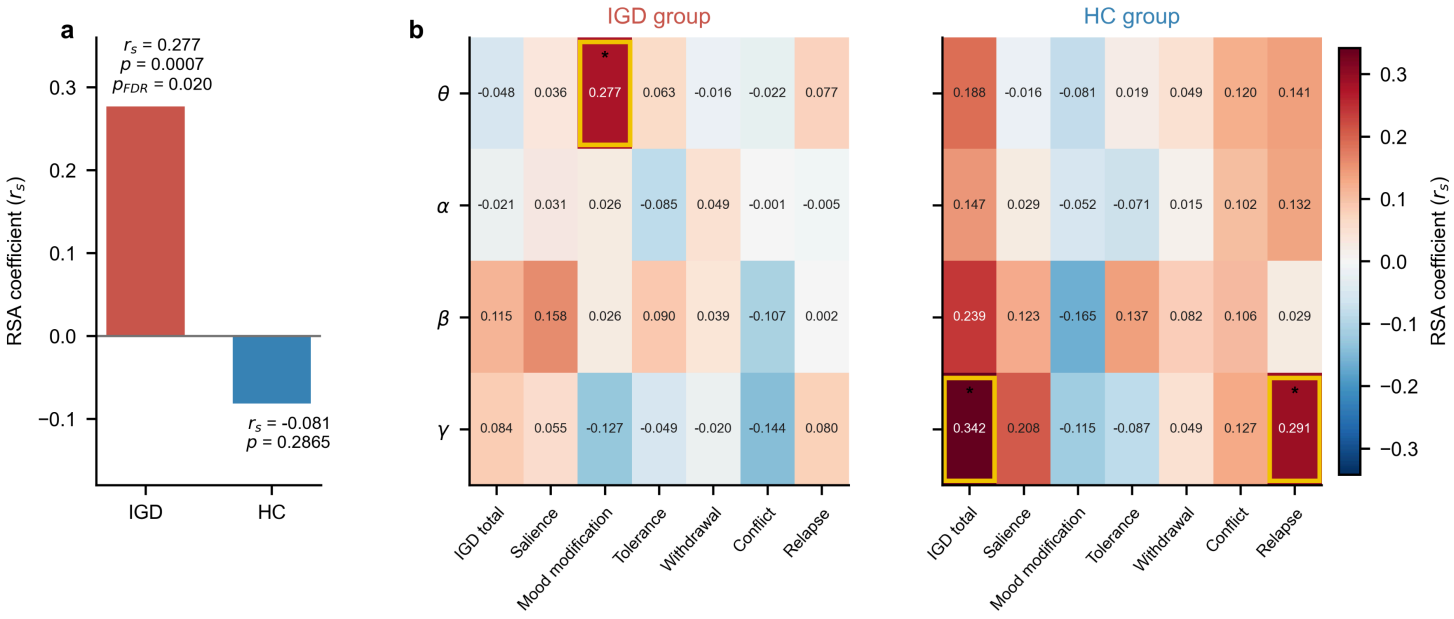


Figure 3

Within-group RSA associations between AEC connectivity profiles and IGD-20 scores. (a) RSA coefficients for theta-AEC connectivity dissimilarity and mood-modification score dissimilarity in each group. (b) RSA coefficients across four frequency bands and seven IGD-20 variables. Highlighted cells survived FDR correction across 28 tests within the corresponding group.

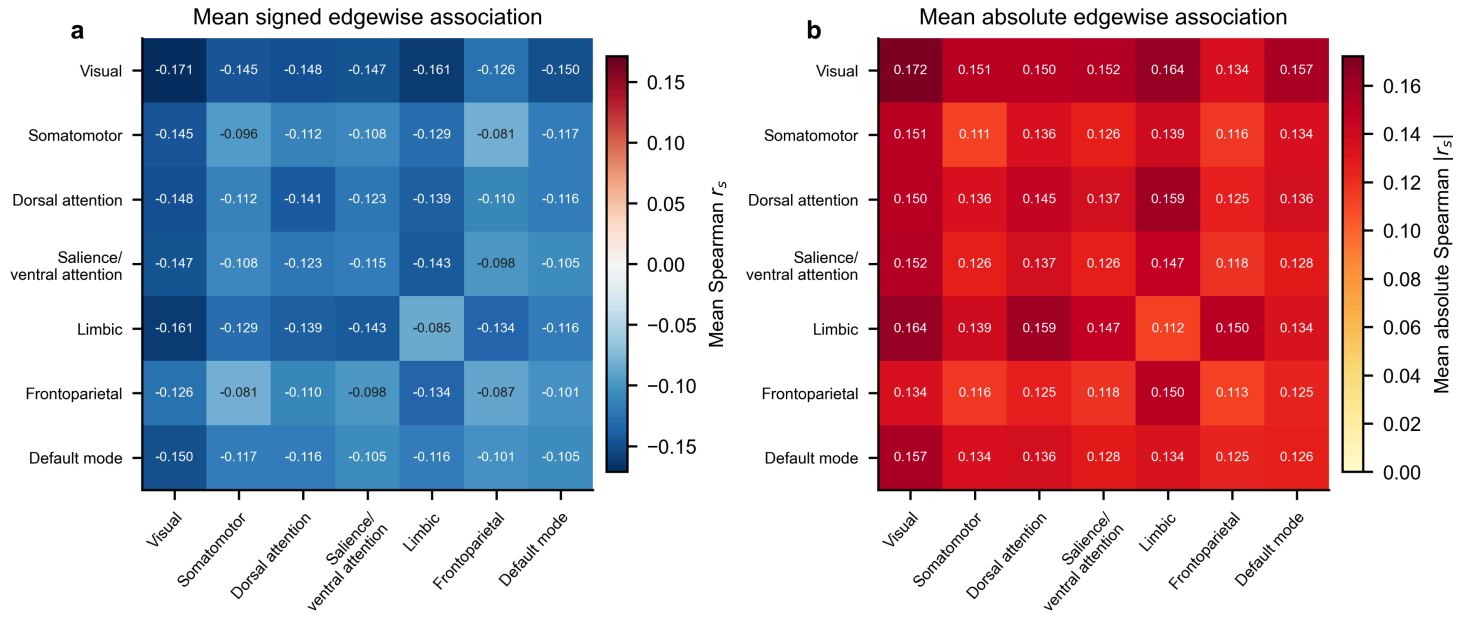


Figure 4

Descriptive network summary of edgewise theta-AEC associations with IGD-20 mood-modification scores. Within the IGD group, Spearman correlations were calculated between each connection's AEC values and mood-modification scores across participants. Cells show mean signed correlations (a) and mean absolute correlations (b) across connections within or between the seven large-scale networks. Diagonal cells summarize unique within-network connections, excluding self-connections. These network summaries are descriptive; no individual connection survived FDR correction across 4950 tests.

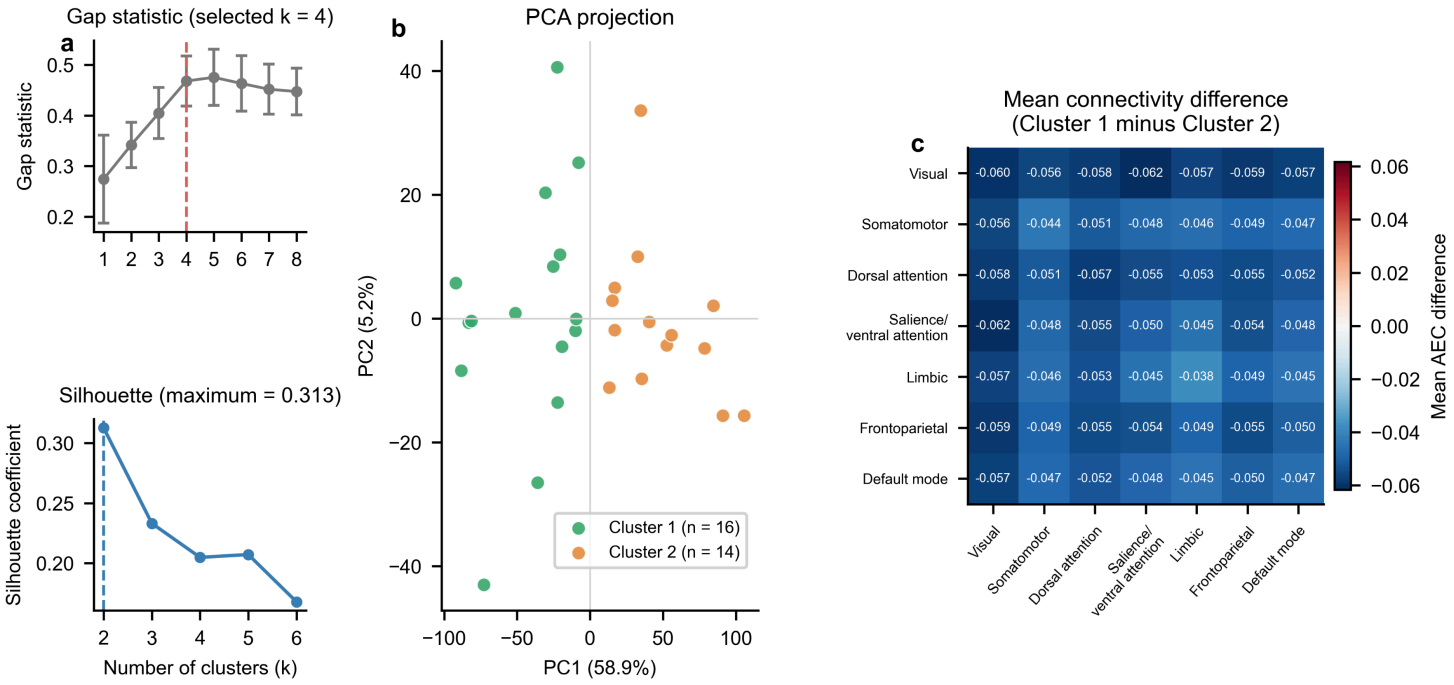


Figure 5

Exploratory two-cluster representation of theta-AEC connectivity profiles in the IGD group. (a) Cluster-number evaluation using the gap statistic for k = 1–8 and the mean Silhouette coefficient for k = 2–6. The gap statistic selected k = 4, whereas the Silhouette coefficient was highest at k = 2. Error bars for the gap statistic show the reference-distribution uncertainty term used by the selection rule. (b) Projection of participants onto the first two principal components, which explained 58.9% and 5.2% of the variance, respectively. Colors indicate the two-cluster assignment obtained in the PCA-reduced space using 23 components that collectively explained 95.2% of the variance. (c) Post hoc differences in mean theta-AEC connectivity within and between the seven large-scale networks, calculated as Cluster 1 minus Cluster 2. Panel c is descriptive and does not represent an independent statistical comparison.